Desy Summer Student Program 2016

Hamburg

Estimation of the TFR scale factors for the $e-\tau$ channel and deriviation of the QCD with a data-driven method for the $\mu-\tau$ channel.

Georgios Polykratis[1]

National and Kapodistrian University of Athens

Supervisor: Alexis Kalogeropoulos[2]
Desy

September 7, 2016

[1]giopolykra@protonmail.com
[2]Alexis.Kalogeropoulos@cern.ch

Abstract

At the first part of the analysis we estimate the tau miss identification rate of for the $e - \tau$ channel. The scope of this analysis is the derivation of a scale factor with which we will reweigth the number of monte carlo (MC) generated events, that accounts for the tau miss identification. On the second part we present the results of the agreement between the monte carlo bkg and the data at the signal region and we attribute the discrepancy to the MC QCD. We then derive the QCD bkg using a data-driven method for the $\mu - \tau$ channel and compare our results with the previous ones for the MC QCD. Finally propose extra cuts for various kinematic variables in the signal region in order to increase the signal over bkg.

Contents

1 Introduction

1.1 Scope and Motivation

The primary scope of this analysis is to increase the agreement between the data and the monte carlo in the signal region, the definition of which will be given at section 3. We chose two ways to achieve a correction to the Monte Carlo. The first is to estimate the rate of the tau miss identification and rescale the data by a respective parameter, called tau fake rate scale factor (TFR s.f.), and the second is to derive the QCD using a data driven method.

1.2 Variables

1.2.1 Transverse Momentum

As transverse momentum of an object we define the magnitude of the projection of the momentum on the transverse plane:

$$p_T = \sqrt{p_x^2 + p_y^2}$$

1.2.2 Missing Transverse Momentum and Energy

To properly account for the particles like neutrinos and weakly interacting stable particles that escape direct detection, we use the variable of missing energy. It is defined as the energy imbalance of the final state and it can be expresses as a vector or a scalar variable. The vector definition of the missing energy, which is often called missing transverse momentum is given by the negative sum of the transverse momentum of all the the final state objects of the event (enumerated by the index i):

$$\not\boldsymbol{E}_{\boldsymbol{T}} = -\sum_i \boldsymbol{p}_{\boldsymbol{T}}^{\boldsymbol{i}}$$

The respective scalar definition, is called missing transverse energy and is given by the formula:

$$\not{E}_T = \sqrt{(\sum_i E_x^i)^2 + (\sum_i E_y^i)^2}$$

where the index i refers to the i-th object of the event.

1.2.3 Transverse Mass

The transverse mass of the missing energy and the lepton is defined as:

$$M_T = \sqrt{2 p_{T,\ell}\ p_{T,\not{E}_T} \left(1 - \cos\Delta\phi(\ell, \not{E}_T)\right)}$$

1.2.4 Impact Parameters

The impact parameters (IP) are variables used to distinguish the decay products of prompt tracks. The fact that massive particles travel through the detector a certain distance before they decay into something else, leads to the creation of secondary vertices. The impact parameters are used to identify the relative position of these secondary vertices to the primary vertices.
Two variables are used to specify the relative position of the two vertices. The first is the d_z which gives the distance of the secondary vertex from the primary vertex along the beam axis. The second variable is the d_{xy} which gives the radial distance of the secondary vertex from the z axis.

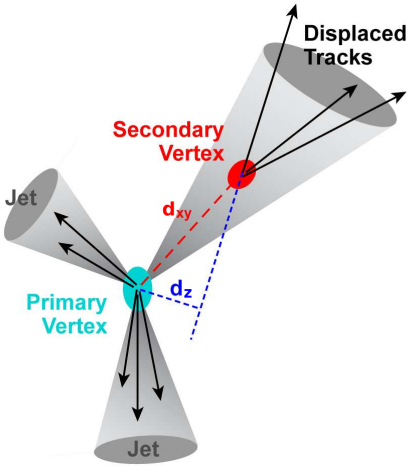

Figure 1: The impact parameter

1.3 Relative Isolation

Charged leptons from the decay of W bosons, as well as the new physics we are searching for, are expected to be isolated from other activity in the event. We calculate a relative measure of this isolation denoted as RelIso.

The relative isolation of an object is measured by comparing the scalar sum of transverse track momenta and transverse calorimeter energy deposits within a cone of $\Delta R = \sqrt{(\Delta\eta)^2 + (\Delta\phi)^2}$ around the lepton candidate direction at the origin, to the transverse momentum of the candidate [1]. The vertex of the cone is the the birth point of the muon or in other words the secondary vertex of the leptonic tau decay. In the current analysis the relative isolation variable for the muons is defined as [2]:

$$RelIso_{\mu} = \frac{\sum p_{T,h} + max\left(0, \sum p_{T,\gamma} + \sum E_{T,h^0} - 1.5 \sum E_{T,pu}\right)}{p_{T,\ell}}$$

where $\sum p_{T,h}$ is the sum of all the hadronic objects inside the cone, $\sum E_{T,\gamma}$ is the sum of transverse momentum of photons inside the cone and $\sum E_{T,h^0}$ is the sum of the missing energy over the neutral hadrons. The last term in the numerator gives the correction of pileup effects by subtracting the contribution from charged particles, originating from pileup vertices. In the numerator we can see that the p_T of the lepton is not summed and for that reason the numerator is called isolation. That way, by demanding the Isolation of the lepton to have a small number we basically select a lepton well isolated inside the cone.

1.3.1 Rapidity

The CMS detector user a right-handed Cartesian coordinate system, with z-axis being along the direction of the beam, y-axis pointing vertically upwards from the center of the detector and x-axis being horizontal, starting from the same point. Because of the cylindrical symmetry of the detector, the coordinates (ρ, ϕ, θ) can be used. Instead of the polar angle θ we use the variable *pseudorapidity* (η) which is invariant under Lorentz boost in the beam direction:

$$\begin{aligned} \eta &= -\log(\tan(\theta/2)) \\ &= \frac{1}{2}\frac{|p| + p_z}{|p| - p_z} \end{aligned}$$

The geometry of the detector sets a limit on the rapidity coverage for the various particles at angles close to the beam line.

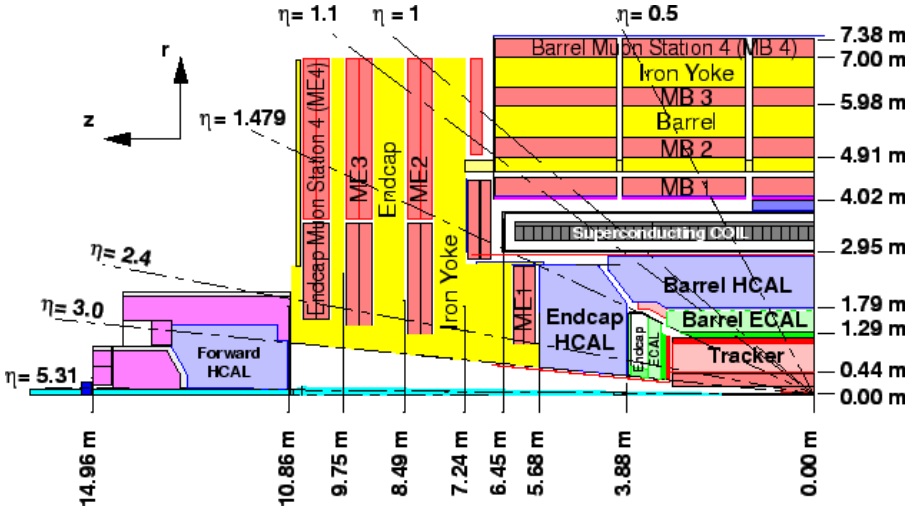

Figure 2: Rapidity coverage of CMS detector

1.4 Process Topology

Our analysis applies for a semi-lepotonic final state $\ell - \tau$, where ℓ can be either a μ or e and the τ is later decayed into hadrons. For this reason the final state τ is also referred to as τ_h. We focus on three different SUSY processes, which all of them include the production of two staus. Those are the direct stau production, the chargino neutralino production (C1N2) and the chargino - chargino production (C1C1).

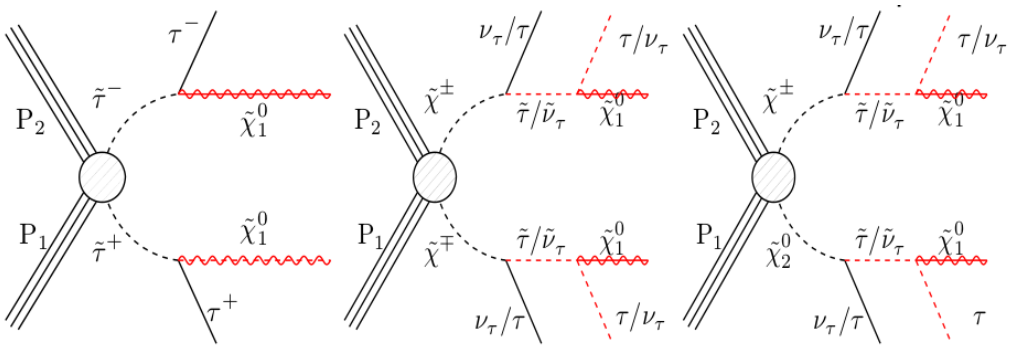

Figure 3: Topology of the three di-stau production channels

The branching ratio of each one of the three possible final states is given in the next table.

From the topology of those processes we see that for the direct di-$\tilde{t}$ production we get opposite charge pair of μ and τ_h, while the other two processes $\tilde{\chi}^\pm\tilde{\chi}^\mp$ and $\tilde{\chi}^\pm\tilde{\chi}^0$ can either give a same or opposite charge pair of μ and τ_h.

Channel	Signature	$\mathcal{BR}$
0-l	$2\tau_h + \not{E}_T$	$0.65^2 = 0.42$
1-l	$\tau_h\tau_l + \not{E}_T$	$2 \times (0.35 \cdot 0.65) = 0.46$
2-l	$2\tau_l + \not{E}_T$	$0.35^2 = 0.12$

The motivation behind this study is that all of these processes have small cross sections, especially the direct stau production because it is part of the family of the slepton production which bears the least cross section among the different possible SUSY processes. As it can be seen in Figure 2, the cross section of the $(\tilde{\tau}\tilde{\tau})$ for a certain SUSY particle mass is 2 orders of magnitude smaller than the cross section of $(\tilde{\chi}^\pm\tilde{\chi}^\mp)$ or $(\tilde{\chi}^\pm\tilde{\chi}^0)$.

With the RUN II data of the LHC we start to have enough data to probe these models.
In this analysis we use CMS data of proton - proton collision with a center of mass energy at 13TeV and total integrated luminosity of 16 fb^{-1}, calculated over the whole data sample.

The event samples we used on the TFR analysis were selected with the use of the trigger:

- HLT_Ele25_WPTight_Gsf

The event sample used for the QCD estimation was selected with the use of the trigger:

- HLT_IsoMu22

The list of data samples that we used are listed in Table 3 and the list of Monte Carlo Samples are listed in Table 4 on the Apendix.

Figure 4: Cross Section Diagramm of SUSY processes

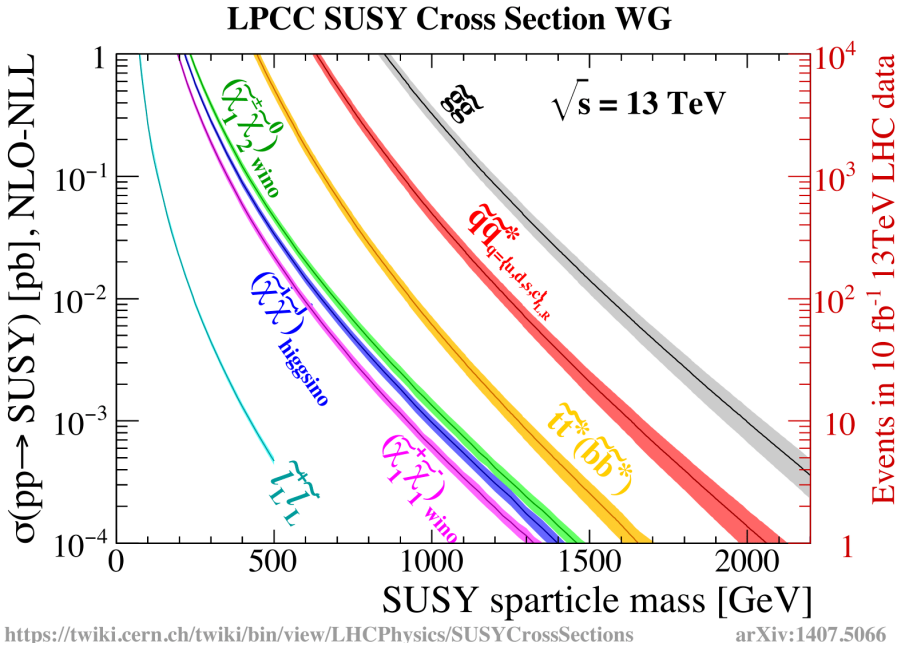

2 Tau Fake Rate Reconstruction

2.1 Event preselection

A number of the events that pass the initial selection criteria for the tau-id does not correspond to real taus. This is due to the fact that jets can be missidentified as hadronicaly decaying taus by the reconstruction algorithm. We want to estimate the rate of jets faking taus (TFR) in order to correct number of the MC generated events.
The major sources of jets which can fake taus are jets produced in QCD processes and jets produced in association with Z and W bosons [3].

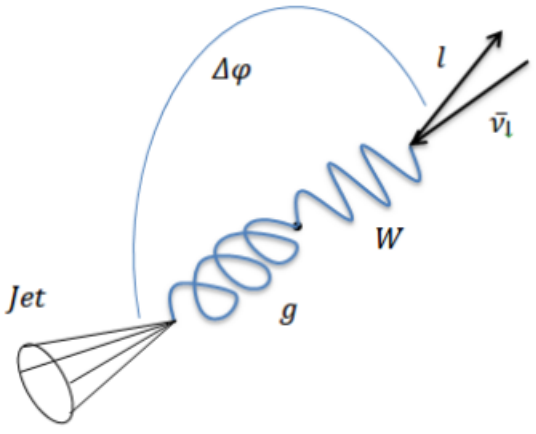

Figure 5: Back to back tag jet plus probe lepton

In this analysis we select a data region enriched with W+Jet events. In this region jets rarely descend from real taus thus this region is considered to be orthogonal to the Signal Region (SR). This process serves as a good candidate for this analysis since the W bosson later decays to a lepton and its neutrino and thus offers a final state similar to the one we investigate (isolated lepton + jets).

These W + Jet events were selected with one isolated electron passing the identification criteria:

- $p_T > 26$ GeV
- $|\eta| < 2.3$
- $d_{xy} < 0.045$ cm
- $d_z < 0.2$ cm
- RelIso < 0.3

Also electrons have to as to match trigger object within $\Delta R < 0.5$. As jets at the proposed test process we define the leading jets, while the W bossons are reconstructed from a lepton and $\not{E}_T$ (that correspond to the same flavour neutrino).

Because of the data sample we are using is W+Jets enriched, the objects that are identified as taus will be miss identifications so a measurement of the respective rate will be a first estimation of the TFR.

2.2 Loose and Tight Tau ID

We separate the objects that our algorithm identifies as taus, into two categories, loose and tight selected taus according to the criteria bellow:

Loose ID:

- $P_t > 20$ GeV
- $|\eta| < 2.3$
- $|d_z| < 0.2$ cm
- Opposite relative Sign to the hadronic jet

Tight ID:
We demand that the taus labeled as tight to satisfy the loose ID criteria and also pass the tauID selection of our algorithm.

The TFR for the data and the MC are defined as $\mathcal{R}_{Data} = \frac{\#Tight}{\#Loose}$ and $\mathcal{R}_{MC} = \frac{\#Tight}{\#Loose}$ respectively, and are use to estimate the tau fake rate scale factor (TFR s.f.).

We define as TFR s.f. the fraction of the the above two rates:

$$\text{TFR s.f.} = \frac{\mathcal{R}_{Data}}{\mathcal{R}_{MC}} = \frac{\frac{Tight}{Loose}\,(Data)}{\frac{Tight}{Loose}\,(MC)}$$

2.3 Further optimization of the W+jets purity

An optimization of the TFR estimation can be established with a sample of increased purity on W+Jets. To maximize the purity of the W+Jets sample we impose four sequential cuts that we apply doth on tight and loose selected taus:

- $\not{E}_T > 40$ GeV
- 60$< M_T <$ 120 GeV
- $\Delta\phi$ >2.5
- $RatioSum = \frac{P_T(W)-P_T(Jets)}{P_T(W)+P_T(Jets)} < 0.2$

The 3rd cut for the lepton - jet separation is equivalent with demanding the descended leptons to be are back to back with the Jets.

2.4 TFR scale factors

After the application of the four sequential cuts, we get the TFR for three different η bins. The parametrization of the η coverage into 3 different bins is characteristic for the $e-\tau$ channel and has to do with the geometry of the detector.

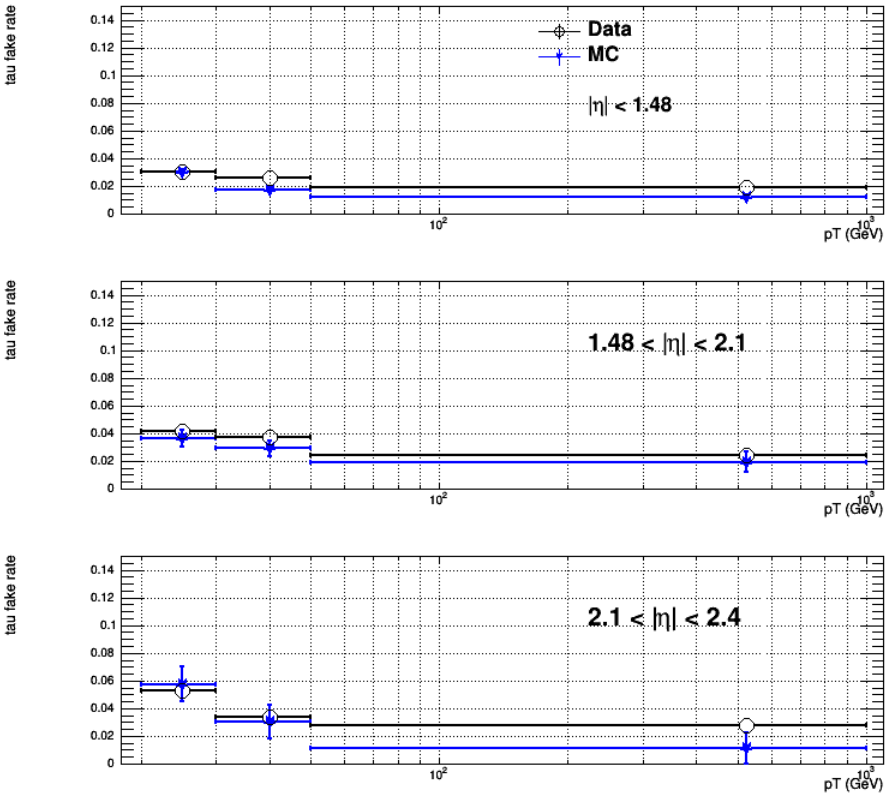

Figure 6: The TFR for three η bins

The scale factors are obtained from the division of the data and monte carlo TFR of the above plot. The resulting scale factors are used to correct the MC generated events for different p_Ts.

3 QCD Estimation

3.1 Event Selection

The reconstruction and identification of physics objects follows official recommendations. The measurements of jets and MET make use of candidates reconstructed with the use of the particle flow (PF) algorithm [[5], [6]]. The PF algorithm combines information from all subdetectors in order to identify leptons, photons as well as charged and neutral hadrons.

3.1.1 μ definition

We impose certain quality cuts on the kinematic variable p_T and the impact parameters of the particles and jets in order to select events of interest.

- $d_{xy} < 0.045$ cm in the transverse plane
- $d_z < 0.2$ cm along the beam axis

The muons are required to have a threshold of $p_T > 23$ GeV and $|\eta| < 2.4$.
In the current analysis the selected relative isolation of the muon is taken to be $RelIso_\mu < 0.15$

3.1.2 τ definition

For the tau collection we select the candidates to have a transverse momentum threshold of $p_T > 20$ GeV and a rapidity threshold of $|\eta| < 2.3$. Also for the impact parameters we impose a restriction only on the beam axis $d_z < 0.2$.

3.1.3 jet definition

For the case of jets the traverse momentum threshold of $p_T > 20$ GeV is imposed. We also set a restriction to the rapidity $|\eta| < 2.4$, and the size of cone definition for the jets $\Delta R < 0.5$.

3.1.4 Extra lepton vetoes

Because the signal we want to investigate has only one lepton in the final state, we impose further vetoes to eliminate the presence of other leptons in the vicinity of the prompt lepton of our selection. For that reason we choose to reject events that pass the following selection:

- $p_T > 10$ GeV
- $|\eta| < 2.4$ for μ 2.3 for e
- $d_{xy} < 0.045$ cm
- $d_z < 0.2$ cm
- RelIso < 0.3

The above restrictions are referred in the bibliography as 3rd lepton vetoes.

Since we work for the $\mu - \tau$ channel, we also need to reject events that pass the selection of a second isolated muon. These are the di-μ vetoes:

- $p_T > 15$ GeV

- $|\eta| < 2.4$
- $d_{xy} < 0.045$ cm
- $d_z < 0.2$ cm
- RelIso < 0.3

4 Trigger Efficiency and Lepton SF

4.1 Trigger Efficiency

Our monte carlo generated events have to be reweighted with a factor that takes into account the detection limitations of the tracker. Because the trigger efficiency plot has to do only with data, the reweighting of the MC events has been done using only the efficiency of the data.

4.2 Lepton Scale Factors

The trigger performance differs between data and monte carlo simulation and thus there are two different efficiency plots of the lepton reconstruction for different transverse momentum of the muon. In order to account for this difference between the efficiencies, we apply the so called lepton scale factor to the MC generated events:

$$LSF = ID\left(\frac{Data}{MC}\right)$$

which is the fraction of the Data over the MC events that pass the lepton ID selection (with objects identified as leptons).

5 Analysis with MC QCD

Using the MC Bkg datasets of Table 2 we plot the histograms of certain kinematic variables. The discrepancy between Data and MC is very noticeable in all variables and especialy for the impact parameters of the μ as shown in Figure 7.

The table bellow shows the cutflow of the events after certain cects and scale factors have been imposed:

TABLE 1: *Cut Flow with MC QCD*

cutflow	**TTJets**	**WJets**	**DYJets**	**QCD**	**SingleT**	**VVJets**	**TTXJets**	**Bkg**	**Unct**	**RelDiff**	**Data**
mu-tau	36093	180483	150604	109497	4802	9814	94	491387	701	-0.493	329190
2nd lepV	35819	180483	139909	109278	4779	9290	88	479647	693	-0.512	317181
3rd lepV	32540	180305	137077	106704	4432	8686	74	469817	685	-0.522	308633
Trigger EF	28154	153488	115356	86164	3833	7420	64	394479	628	-0.278	308633
Lepton SF	27620	150253	112338	83701	3759	7263	63	384997	620	-0.247	308633

The mu-tau selection also includes the the Tau-id which are a correction to the top-quark-pair cross section and an algorithm for the reconstruction of taus that are produced in decays of boosted particles respectively.

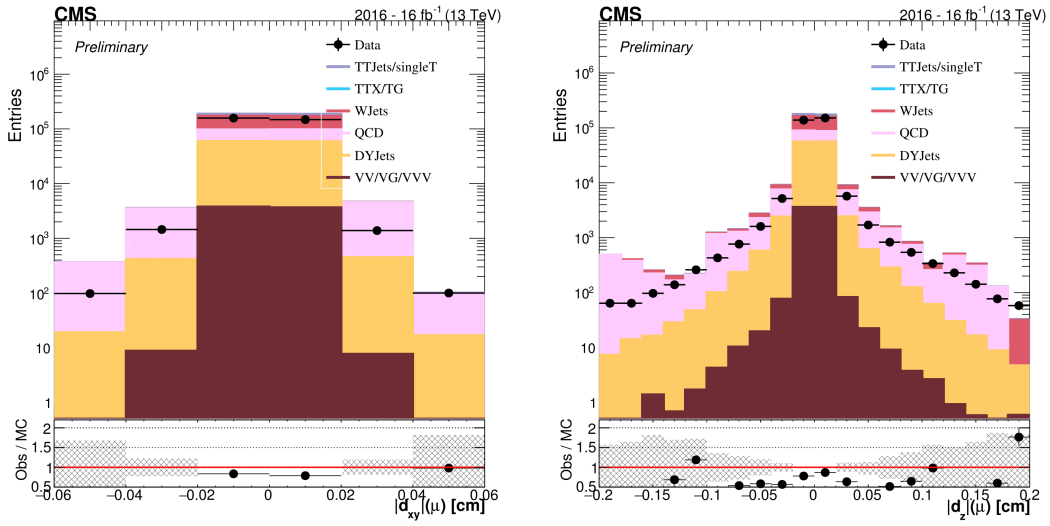

(a) d_{xy} (b) d_z

Figure 7: Muon impact parameters

The 2nd and 3rd lepton Vetoes have been mention in Section 3.4.

The correction of generated events with the Trigger Efficiency has to do with the fact that the reconstruction of objects from the trigger has limitations and is not 100% accurate as the name also indicates. The respective correction to the events is taken into account by a weighting factor which is the product of the Data with the efficiency.

The Lepton scale factor corrects the MC generated events by calculating the fraction of the number particles that have passed the lepton ID selection in the data over that of the MC and using this to re-weight all the events.

As we can see from the cutflow table, after the application of all scale factors the relative difference between Data and MC is 24.7%. This can be attribute to the high cross section of the QCD. Indeed this corresponds to high scaling weights, which combined with the relatively low statistics of our sample (small for the MC estimation of the QCD) give us an estimation for the MC QCD much higher than the true number of events.

It becomes clear that the unsatisfactory statistics makes the monte carlo analysis for the QCD unsatisfactory since it has the greatest cross section from the rest of our MC samples and therefore is liable for the overestimation of the bkg.

The need for a new method of deriving the contribution from the QCD, by surpassing the problem of low statistics becomes evident.

6 Analysis with Data Driven QCD

6.1 Estimation of the QCD with a data-driven method

Because of the inefficiency of the MC generated QCD, we will derive the QCD explicitly from the data and the rest of the MC datasets. This of course cannot be done in the signal region

because this is the region which we want to correct, and any effort of correcting it with the use of data from the same region will contaminate it with bad statistics. So the data-driven way we will use to properly model the QCD will have to make use of data disjoint from the one used for the statistical analysis.

For that lesion we try to use the data and monte carlo from 3 independent regions to estimate the QCD in the Signal Region. This is called the ABCD method. The idea is to use two weakly correlated variables in order to separate the data into 4 orthogonal regions namely A, B, C and D as can be seen in the picture bellow.

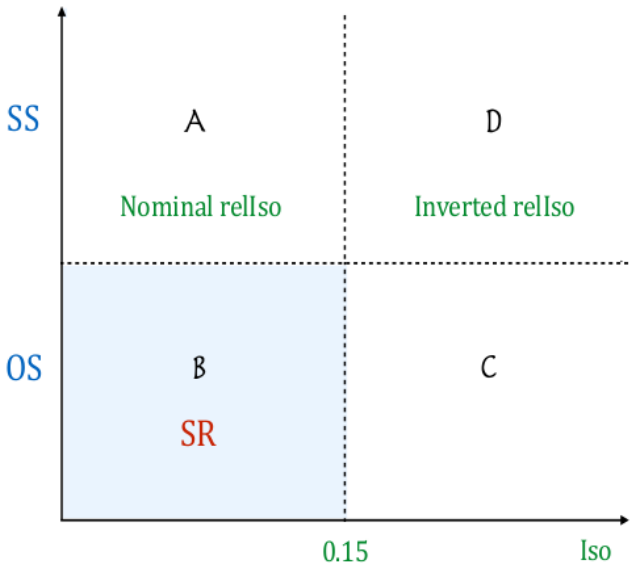

Figure 8: ABCD regions derived with the use of two weakly correlated variables

The product of the diagonal regions are considered to have similar properties and consequently follow similar distributions. The respective mathematical expression $\frac{A}{B} = \frac{C}{D} \rightarrow B = A\frac{C}{D}$ can be used to estimate the desired quantity in the signal region, and in our case the QCD bkg.

The two variables that we choose to separate the data region are the relative Isolation of the muon and the relative charge of the muon and the τ_h. The two of them don't show any indication of linear correlation, as we can see at Figure 9 and thus are taken to be uncorrelated. As it was shown at section 3 the RelIso of the muon for the signal region is selected to be RelIso$<$ 0.15. So it makes sense to pick as a relative isolation for the separation of the data region greater or equal to the RelIso for the Signal Region. We selected the maximum isolation at the B region to be equal to the maximum isolation of the Signal region, in order not to leave any data unused.

The four regions that are created by our data separation cuts are:

- A: SS, $ISO_\mu < 0.15$
- B: OS, $ISO_\mu < 0.15$
- C: OS, $ISO_\mu < 0.15$
- D: SS, $ISO_\mu > 0.15$

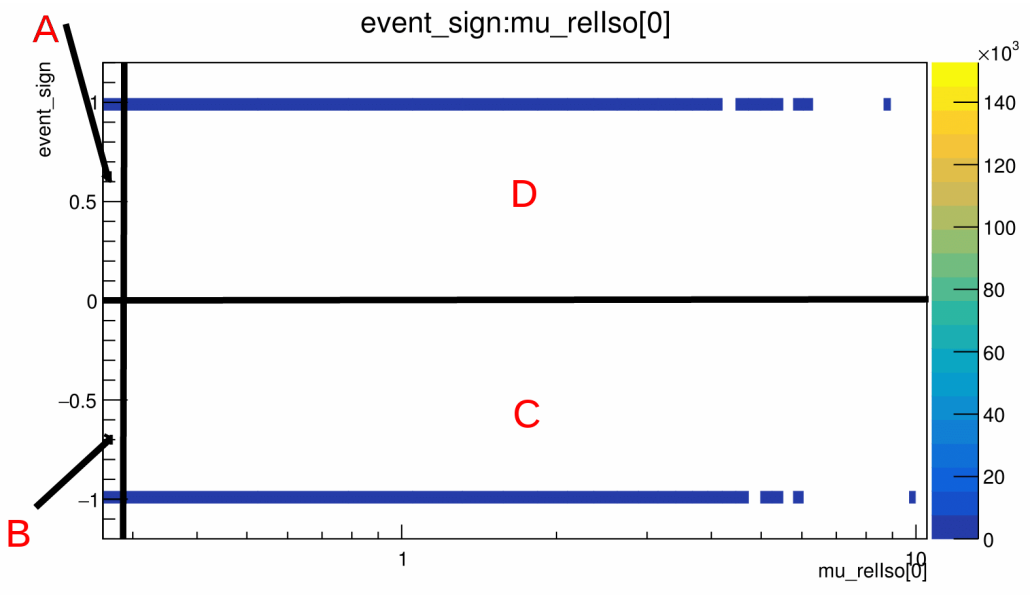

Figure 9: The ABCD regions with plotted events (Data-MC)

The events with which the diagram is filled are derived by the subtraction of the MC generated events (all the datasets except from the MC QCD) from the real data, that is $N_i = N_{Data} - N_{MC}$,with $i = A, B, C, D$ indicating the respective region. That way our estimation of the QCD for the signal region is obtained after a scaling of the region A events over a factor, which is the ratio of events of the other two regions, $N_B = N_A \frac{N_C}{N_D}$.

6.2 Comparison Data Driven QCD vs Monte Carlo

After estimating the QCD with the method described previously, we create plots of the kinematic variables. Now a comparison between the two methods can be made.

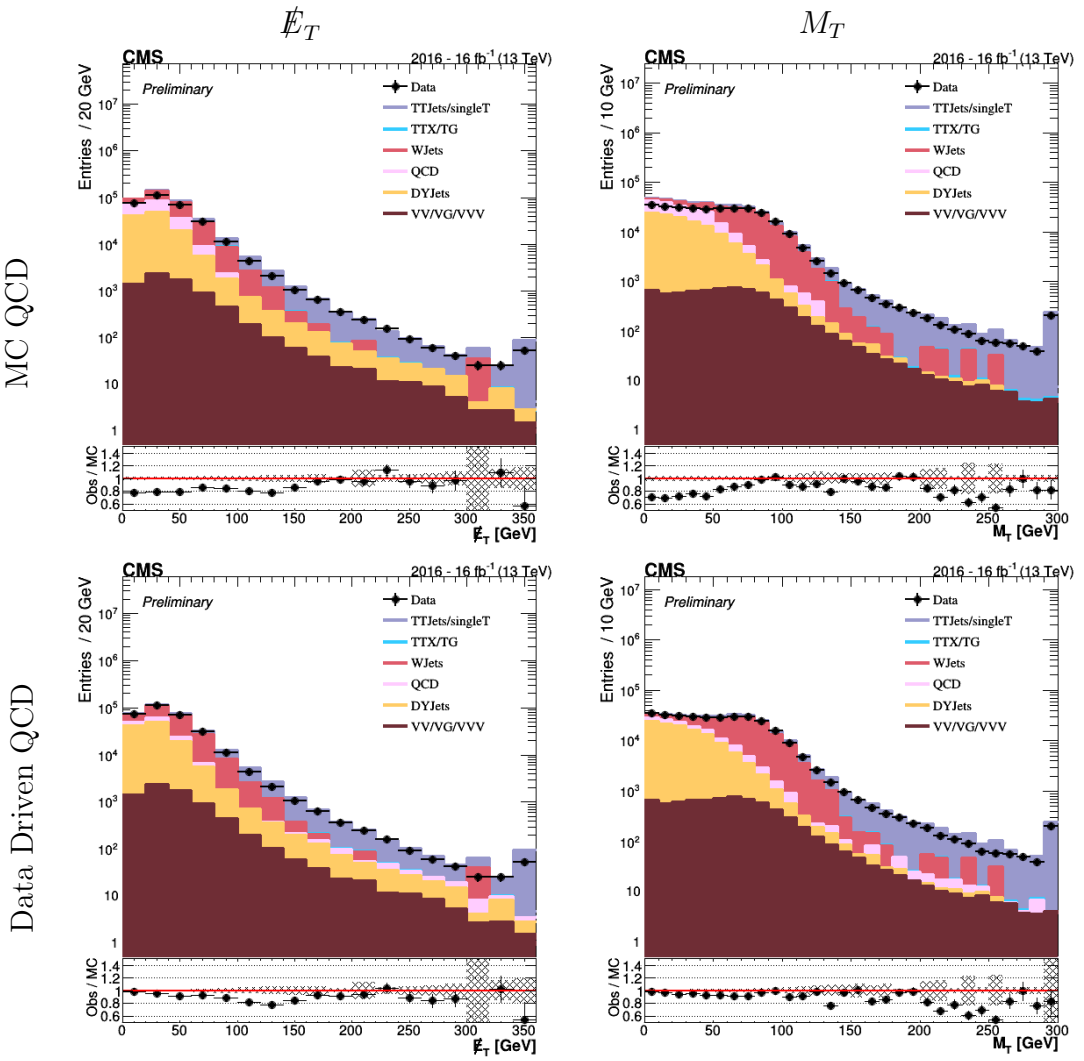

FIGURE 10: *Data-driven vs MC QCD for the $\not{E}_T$ and M_T*

From the MET and M_T plots we can see that a better agreement at the low energy region has been established. This is the region were we have the most qcd contribution, because in general the products of qcd don't have great values of momentum.

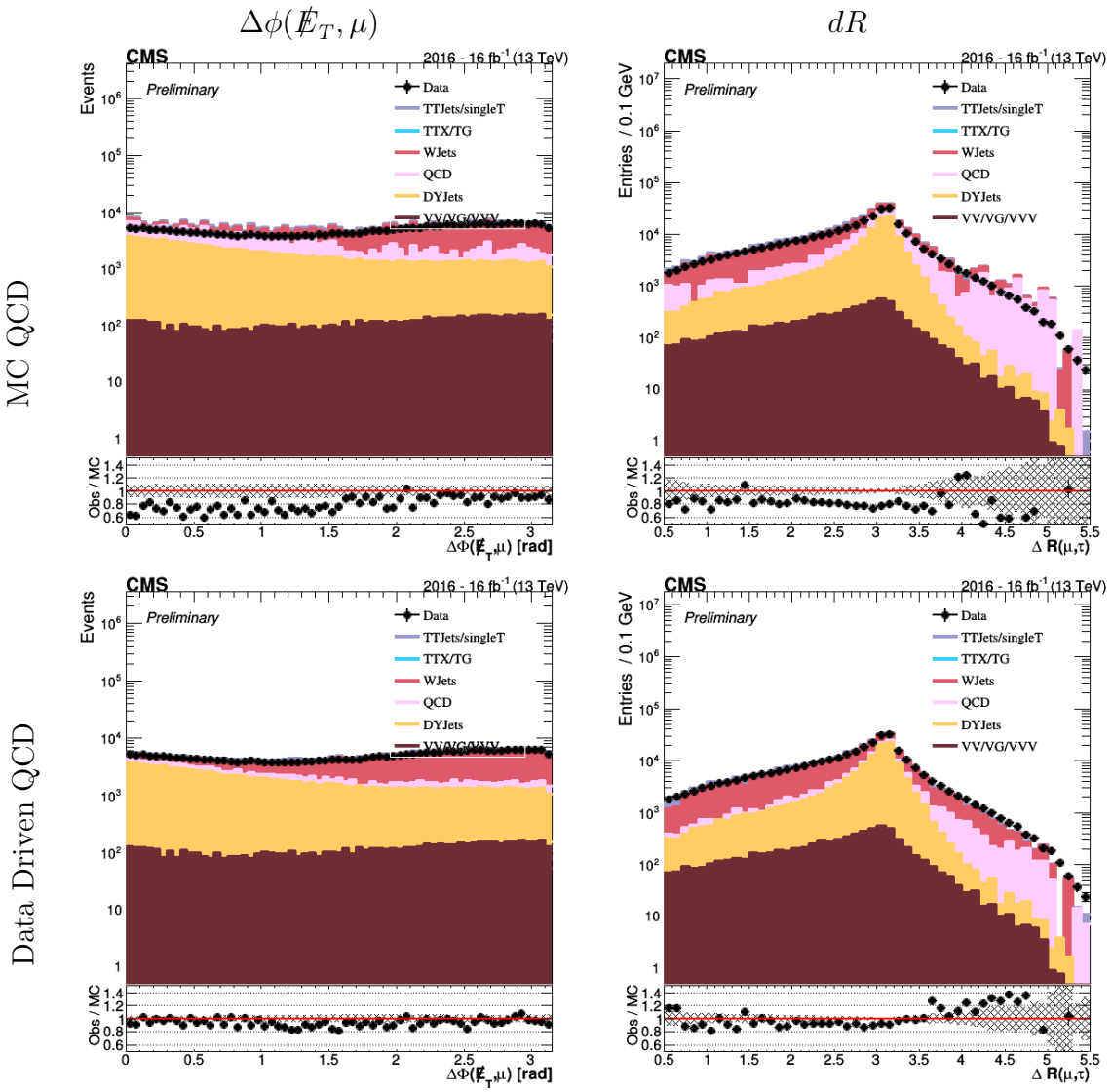

FIGURE 11: *Data-driven vs MC QCD for the* $\Delta\phi(\not{E}_T, \mu)$ *and* dR

In the case of the $\Delta\phi$ we observe that although the QCD contribution is almost homogeneous in all the angles, with the Data Driven QCD we have an improvement on the shape of the stacked bkg histograms. Also the increased number of entries at higher values of the ΔR has decreased improving the shape of the distribution.

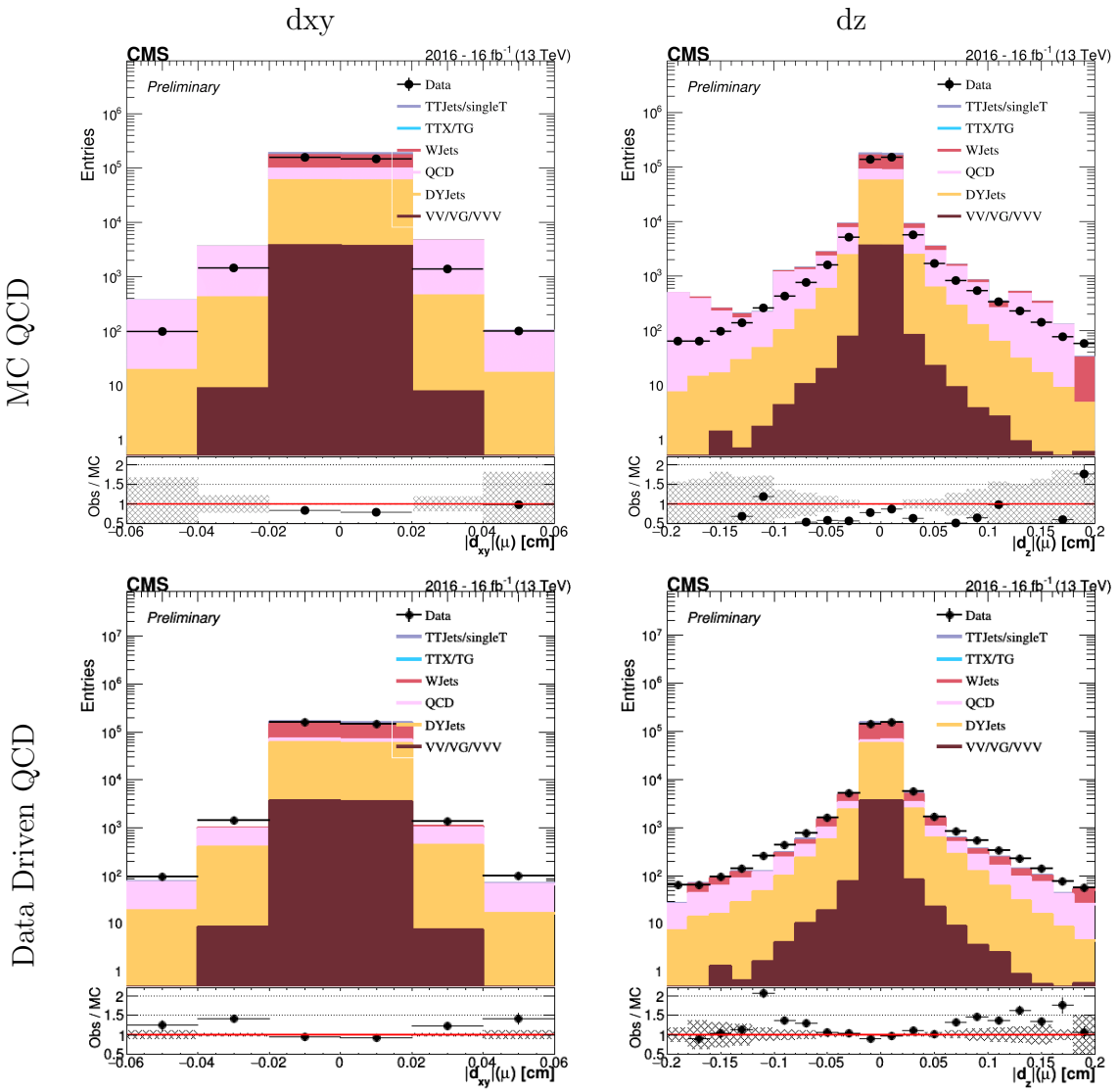

FIGURE 12: *Impact Parameters*
The errors are only due to statistical uncertainties

We can see that the discrepancy of the plots of the impact parameters for the muon has decreased, resulting on a better agreement between data and Monte Carlo.

We reevaluate the cutflow for the Data Driven QCD also including the scaling factor of the TFR. We see that up to the application of the Lepton scale factor, the relative difference between MC and Data is reduced compared to the previous analysis from the value 24.7% to the value 4.9%. With the reweighting of the generated events also by the TFR scale factor the relative difference reduces to 1.7%.

TABLE 2: *Cut Flow with Data Driven QCD and TFR*

cutflow	TTJets	WJets	DYJets	QCD	SingleT	VVJets	TTXJets	Bkg	Unct	RelDiff	Data
mu-tau	36093	180483	150604	15024 ± 74	4802	9814	94	396915	630	-0.206	329190
2nd lepV	35819	180483	139909	15680 ± 194	4779	9290	88	386049	621	-0.217	317181
3rd lepV	32540	180305	137077	15100 ± 192	4432	8686	74	378213	615	-0.225	308633
Trigger EF	28154	153488	115356	21588 ± 203	3833	7420	64	329903	574	-0.069	308633
Lepton SF	27620	150253	112338	22378 ± 291	3759	7263	63	323673	569	-0.049	308633
TauFakeRate	25770	158646	97840	20847 ± 304	3614	7115	61	313892	560	-0.017	308633

6.3 A few words for future research

The next step in the analysis of the three processes we mentioned in the introduction is to compare the bkg with the expected theoretical signal of those processes. In order to do that we plot the signals for the different kinematic variables but scaled by a factor of 10. This is because all of those processes, as we already mentioned, have small cross section, but we still want to determine the regions with the fewer bkg relative to the signal because those will be the regions were future analyses will be conducted. The plots presented bellow have been obtained after the application of the TFR scale factors and using the data-driven QCD.

nJets

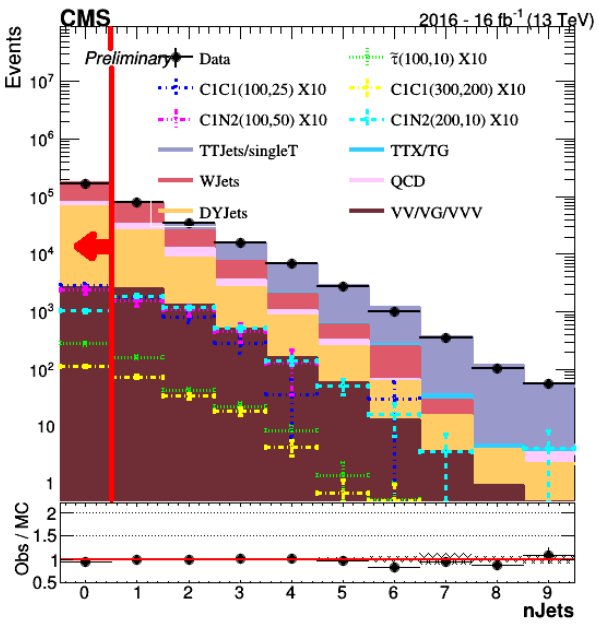

dR

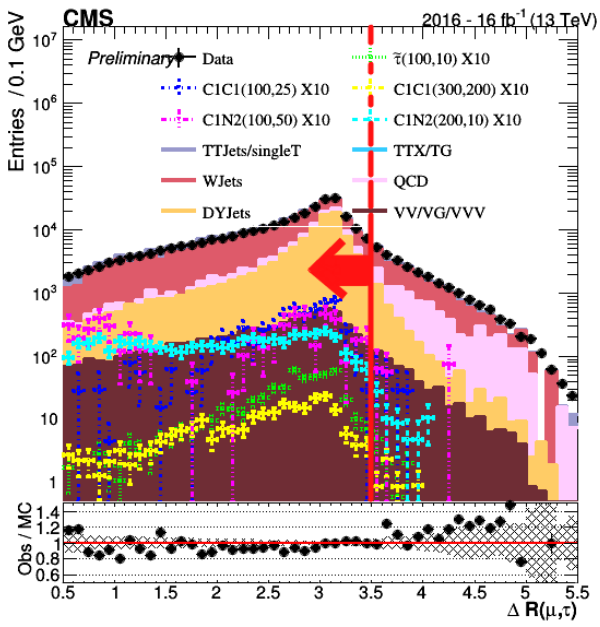

We propose the cut $\#jets = 0$. That is because the signal for all three processes has maximum value for a zero jet final state. Also we will choose to restrict future analyses on ΔR <3.5 region in order to get rid of most of the QCD contribution and also because the signals appear

$\not{E}_T$ M_T

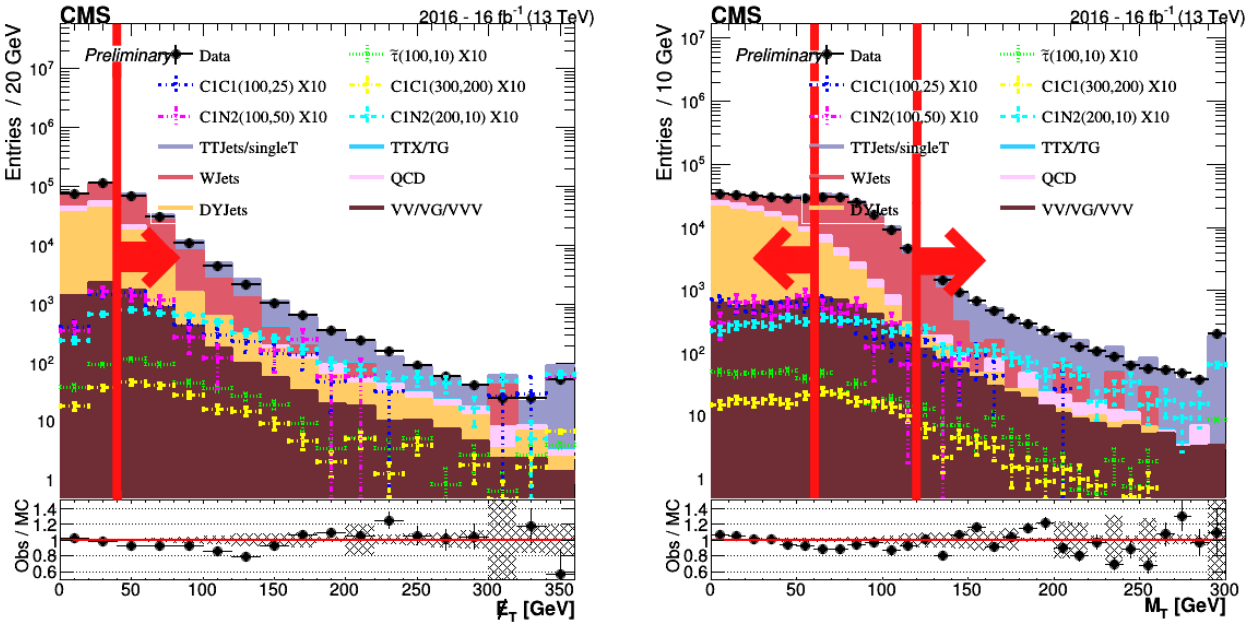

to have decreased values relatively to the bkg.

As for the missing energy, we restrict our analysis on $\not{E}_T > 40$ GeV region, to get reed of the Drell-Yan and QCD contributions of lower regions. Also we exclude the $60 < M_T < 120$ region because of the increased contributions from the weak interactions.

7 Summary

We began with an estimation of the TFR for the e-τ channel using the tag and probe method for a W+jets enriched data sample. Then we moved on to estimate the QCD contribution to the bkg using a data-driven method and we compared our results the the MC generated QCD. Finally we proposed further quality cuts to certain variables for the signal region which future analyses can use.

8 Abstract

8.1 Data and monte carlo samples

TABLE 3: *Datasets*

μ Datasets	e Datasets
SingleMuon_Run2016B-PromptReco_v2	SingleElectron_Run2016B-PromptReco_v2
SingleMuon_Run2016C-PromptReco_v2	SingleElectron_Run2016C-PromptReco_v2
SingleMuon_Run2016D-PromptReco_v2	SingleElectron_Run2016D-PromptReco_v2

TABLE 4: *The simulated MC samples used in the analysis*

	MC Samples	Cross Section (pb)
TT	TT_TuneCUETP8M1_13TeV-powheg-pythia8_ext4-v1	831.76
ST	ST_t-channel_antitop_4f_leptonDecays_13TeV-powheg-pythia8_TuneCUETP8M1	26.38
	ST_t-channel_top_4f_leptonDecays_13TeV-powheg-pythia8_TuneCUETP8M1	44.33
	ST_tW_antitop_5f_inclusiveDecays_13TeV-powheg-pythia8_TuneCUETP8M1	35.85
	ST_tW_top_5f_inclusiveDecays_13TeV-powheg-pythia8_TuneCUETP8M1	35.85
	ST_s-channel_4f_leptonDecays_13TeV-amcatnlo-pythia8_TuneCUETP8M1	3.36
TTX	TGJets_TuneCUETP8M1_13TeV_amcatnlo_madspin_pythia8	2.967
	TTGJets_TuneCUETP8M1_13TeV-amcatnloFXFX-madspin-pythia8	3.697
	TTTT_TuneCUETP8M1_13TeV-amcatnlo-pythia8	0.009103
WJets	WJetsToLNu_TuneCUETP8M1_13TeV-madgraphMLM-pythia8	61526.7
QCD	QCD_Pt-20toInf_MuEnrichedPt15_TuneCUETP8M1_13TeV_pythia8	302672.16
VV/VG/VVV	WGToLNuG_TuneCUETP8M1_13TeV-madgraphMLM-pythia8	489
	WWG_TuneCUETP8M1_13TeV-amcatnlo-pythia8	0.2147
	WWTo2L2Nu_13TeV-powheg	12.178
	WWTo4Q_13TeV-powheg	51.723
	WWToLNuQQ_13TeV-powheg	49.997
	WWW_4F_TuneCUETP8M1_13TeV-amcatnlo-pythia8	0.2086
	WWZ_TuneCUETP8M1_13TeV-amcatnlo-pythia8	0.1651
	WW_DoubleScattering_13TeV-pythia8	1.64
	WZTo1L1Nu2Q_13TeV_amcatnloFXFX_madspin_pythia8	10.71
	WZTo1L3Nu_13TeV_amcatnloFXFX_madspin_pythia8	3.033
	WZTo2L2Q_13TeV_amcatnloFXFX_madspin_pythia8	5.595
	WZTo3LNu_TuneCUETP8M1_13TeV-powheg-pythia8	4.42965
	WZZ_TuneCUETP8M1_13TeV-amcatnlo-pythia8	0.05565
	ZGGJets_ZToHadOrNu_5f_LO_madgraph_pythia8	0.3729
	ZGTo2LG_TuneCUETP8M1_13TeV-amcatnloFXFX-pythia8	117.864
	ZZTo2L2Nu_13TeV_powheg_pythia8	0.564
	ZZTo2L2Q_13TeV_amcatnloFXFX_madspin_pythia8	3.22
	ZZTo2Q2Nu_13TeV_amcatnloFXFX_madspin_pythia8	4.04
	ZZTo4L_13TeV_powheg_pythia8	1.256
	ZZTo4Q_13TeV_amcatnloFXFX_madspin_pythia8	6.929
	ZZZ_TuneCUETP8M1_13TeV-amcatnlo-pythia8	0.01398
	tZq_ll_4f_13TeV-amcatnlo-pythia8	0.0758
	ttWJets_13TeV_madgraphMLM	0.4853
	ttZJets_13TeV_madgraphMLM	0.5124
	WW_TuneCUETP8M1_13TeV-pythia8	63.21
	WZ_TuneCUETP8M1_13TeV-pythia8	47.13
DYJets	DYJetsToLL_M-10to50_TuneCUETP8M1_13TeV-madgraphMLM-pythia8	18610
	DYJetsToLL_M-50_TuneCUETP8M1_13TeV-madgraphMLM-pythia8	6025.2

9 Bibliography

References

[1] S. Chatrchyan *et al.* [CMS Collaboration], "Search for new physics with same-sign isolated dilepton events with jets and missing transverse energy at the LHC," CMS-SUS-10-004.

[2] `https://twiki.cern.ch/twiki/bin/view/CMSPublic/SWGuideMuonId#Muon_Isolation`

[3] [CMS Collaboration], "Performance of tau reconstruction algorithms in 2010 data collected with CMS," CMS PAS TAU-11-001.

[4] [CMS Collaboration], "Search for new physics with same-sign isolated dilepton events with jets and missing transverse energy at the LHC," CMS-SUS-10-004.

[5] [CMS Collaboration], "Particle-Flow Event Reconstruction in CMS and Performance for Jets, Taus, and MET," CMS-PAS-PFT-09-001.

[6] [CMS Collaboration], "Commissioning of the Particle-Flow reconstruction in Minimum-Bias and Jet Events from pp Collisions at 7 TeV," CMS-PAS-PFT-10-002.